Temperature dependence of spectral linewidth of InAs/InP quantum dot distributed feedback lasers

J. Duan[a,*], H. Huang[a], K. Schires[a], P. J. Poole[b], C. Wang[c], and F. Grillot[a,d]

[a]LTCI, Télécom ParisTech, Université Paris-Saclay, Paris, France;
[b]Advanced Electronics and Photonics Research Center, NRC Canada, Ottawa, Canada;
[c]School of Information Science and Technology, ShanghaiTech University, Shanghai, China;
[d]Center for High Technology Materials, University of New-Mexico, Albuquerque, NM, USA

ABSTRACT

In this paper, we investigate the temperature dependence of spectral linewidth of InAs/InP quantum dot distributed feedback lasers. In comparison with their quantum well counterparts, results show that quantum dot lasers have spectral linewidths rather insensitive to the temperature with minimum values below 200 kHz in the range of 283K to 303K. The experimental results are also well confirmed by numerical simulations. Overall, this work shows that quantum dot lasers are excellent candidates for various applications such as coherent communication systems, high-resolution spectroscopy, high purity photonic microwave generation and on-chip atomic clocks.

Keywords: quantum dots, distributed feedback laser, coherent communications, spectral linewidth

1. INTRODUCTION

The combination of advanced modulation formats and coherent detection are the key technologies in coherent communication systems to overcome limitations of current fiber infrastructures.[1] Over the past years, the fast digital signal processing (DSP) technology has been successfully implemented in the fiber transmission system and semiconductor lasers are nowadays used as local oscillators in coherent detection systems. Narrow linewidth lasers are especially important for new systems which use higher-order modulation formats. For instance, at 40 Gbit/s, the laser linewidth must be in the range of 240 kHz, 120 kHz, and 1 kHz for 16PSK, 16QAM, and 64QAM, respectively.[2] To meet these goals, quantum dots (QDs) remain promising candidates owing to the ultimate carrier confinement and the pretty low population inversion factor.[3] For instance, Su and Lester reported an InAs/GaAs QD laser with a linewidth around 500 kHz.[4] Lu et al. demonstrated a linewidth of less than 150 kHz in an InAs/InP QD laser,[5] while Becker et al. achieved a record linewidth of 110 kHz.[6] In this context, our prior work has shown the importance of controlling spatial nonlinearities originating from spatial hole burning for narrowing the spectral linewidth at high drive currents.[7] For instance, using a QD distributed feedback (DFB) laser with symmetric facet coatings has led to spectral linewidths below 400 kHz over a wide range of bias current. In addition, a high degree of stability of the spectral linewidth over temperature is also a very important feature for low-cost and Peltier-free applications. With QD lasers, a temperature insensitive behavior is expected when the sublevel splitting is larger than the thermal activation energy.[8] This work investigates both experimentally and theoretically the temperature dependence of the spectral linewidth of InAs/InP QD DFB lasers. As compared to their quantum well (QW) counterparts, the spectral linewidth is found to be rather insensitive to the temperature. The experimental results are also confirmed by a rate equation model taking into account the spontaneous emission noise and the carrier noise. Overall, this work shows that QD lasers are excellent solutions for narrow linewidth operation which is of first importance not only for coherent communication systems but also for high-resolution spectroscopy, high purity photonic microwave generation and on-chip atomic clocks.

*jianan.duan@telecom-paristech.fr

2. LASER STRUCTURE

The QD gain material was grown by chemical beam epitaxy (CBE) on a (001) oriented n-type InP substrate. The undoped active region of the laser consisted of five stacked layers of InAs QDs with 30 nm $In_{0.816}Ga_{0.184}As_{0.392}P_{0.608}$ (1.15Q) barriers. Each layer contains QDs with an average dot density of approximately 4×10^{10} cm^{-2}. The grating period is 235 nm leading to an operating wavelength of 1.52 μm. The single lateral mode ridge waveguide laser has a cavity length of 1 mm and a stripe width of 3 μm. One of the cleaved facets was coated with a high reflectivity coating of 62%, the other with a low reflectivity coating of 2%. Figure 1(a) represents the light current characteristics for the QD DFB laser for different temperatures ranging from 283 K to 303 K with a step of 5 K. The threshold current is increased from 42 mA at 283K to 52 mA at 303K. Figure 1(b) shows the lasing spectrum operating at $2\times I_{th}$ (293K). Single mode emission is successfully achieved with a side mode suppression ratio (SMSR) of 51 dB. The inset also gives the corresponding SMSR as a function of temperature measured at $2\times I_{th}$, showing that the single mode behavior is enhanced from 50.2 dB at 283K to 52 dB at 303K.

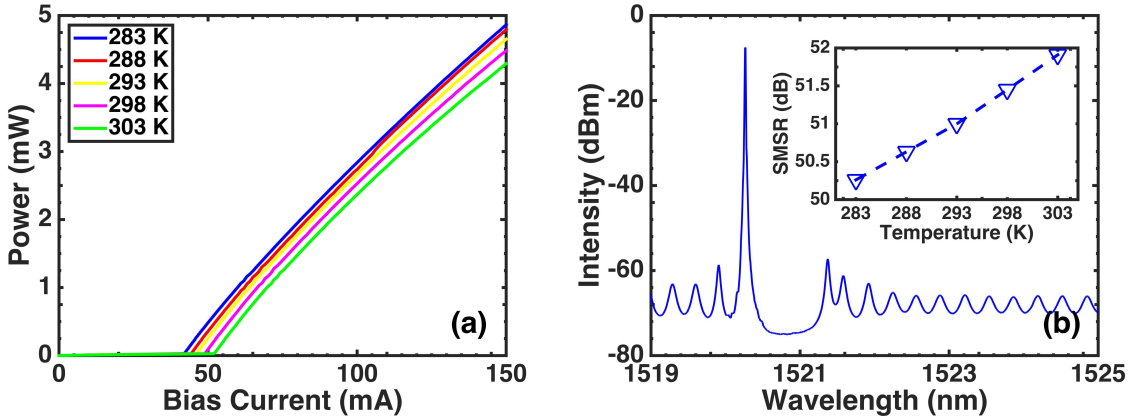

Figure 1. (a) L-I curves measured for different temperatures ranging from 283 K to 303 K. (b) Optical spectrum measured at $2\times I_{th}$ (293K). The inset shows the corresponding variation of the SMSR with temperature at $2\times I_{th}$.

3. EXPERIMENTAL RESULTS

The spectral linewidth is measured with a self-heterodyne interferometric technique incorporating a delay line of 25 km.[9] The intrinsic spectral linewidth has a Lorentzian shape, however, due to the Gaussian shape filter in the electrical spectrum analyzer (ESA) and the residual electrical noise from the power supply as well as thermal fluctuations, the linewidth is rather in the shape of a Voigt function, which is defined as the convolution of a Gaussian function and a Lorentzian function.

In this work, the retrieval procedure is simplified by using a normalized pseudo-Voigt function f_V such as:

$$f_V = (1-\eta)f_G(x,\gamma_G) + \eta f_L(x,\gamma_L) \quad (1)$$

where f_G and f_L are the normalized Gaussian and Lorentzian functions represented as:

$$f_G(x,\gamma_G) = (1/\pi^{1/2}\gamma_G)exp(-x^2/\gamma_G^2) \quad (2)$$

$$f_L(x,\gamma_L) = (1/\pi\gamma_L)(1+x^2/\gamma_L^2)^{-1} \quad (3)$$

where γ_G and γ_L are related to the full-width at half maximum (FWHM) of the Gaussian and Lorentzian functions respectively, and η is the mixing parameter.

In the experiments, the captured radio-frequency (RF) spectrum is the spectral aliasing of both the negative and the positive sides of the full spectral range, hence the output of the ESA is the convolution of two parts, which must be taken into account to retrieve the original spectral linewidth.

As such, the FWHM linewidths from the Gaussian and Lorentzian parts can be expressed as:

$$\Gamma_G = 2\sqrt{\ln 2}\gamma_G \tag{4}$$

$$\Gamma_L = 2\gamma_L \tag{5}$$

The FWHM of the pseudo-Voigt profile can be defined as:[10]

$$\Gamma_V = (\Gamma_G^5 + 2.69269\Gamma_G^4\Gamma_L + 2.42843\Gamma_G^3\Gamma_L^2 + 4.47163\Gamma_G^2\Gamma_L^3 + 0.07842\Gamma_G\Gamma_L^4 + \Gamma_L^5)^{1/5} \tag{6}$$

Figure 2(a) displays the spectral linewidth as a function of the normalized bias current for the QD DFB laser measured at 283K, 293K and 303K, respectively. From the pseudo-Voigt profile, a minimum linewidth of 168 kHz is obtained at 283K ($I/I_{th} = 1.3$). When the temperature is raised to 293K, this minimum slightly increases to 177 kHz ($I/I_{th} = 1.4$) and to 178 kHz at 303K ($I/I_{th} = 1.5$). Overall, the variation of the spectral linewidth does not exceed 5%, which proves the very good stability over the temperature range. A comparison with a commercial QW DFB laser operating at 1.55 μm is also performed. Figure 2(b) shows the evolution of the spectral linewidth of the QW DFB laser assuming the same experimental conditions. Results show that the minimum linewidth is now enhanced from 2.5 MHz at 283K to 3.1 MHz at 303K, which corresponds to a variation of about 23% (600 kHz) over the same temperature range. The minimum linewidth at 303 K is found at lower normalized bias current ($I/I_{th} = 2.5$) than the value at 283K ($I/I_{th} = 3.5$), while it is opposite in QD laser. This effect is attributed to the variation of the threshold current which is about 61% for the QW laser against 23% for the QD one over the same temperature range. In contrast to QW lasers, the spectral linewidths of QD lasers are found much narrower and rather independent of the temperature, which is very promising for aforementioned applications.

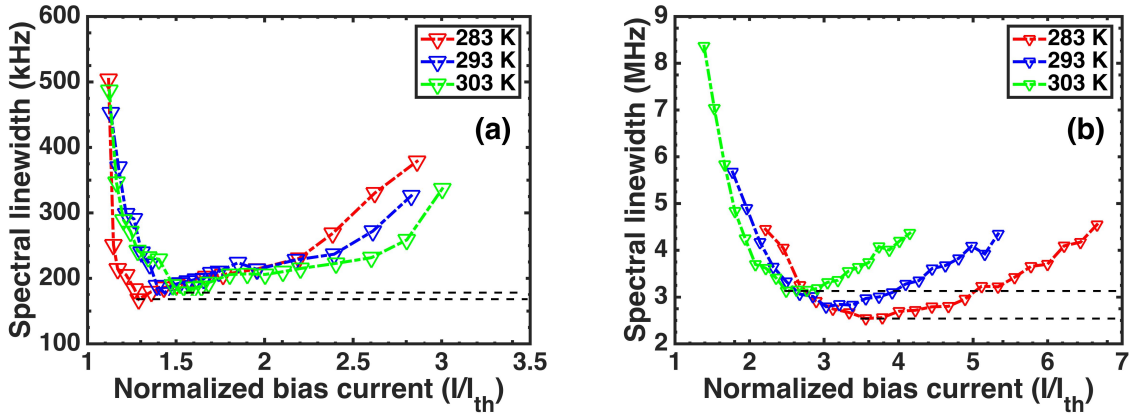

Figure 2. Spectral linewidth of the QD DFB laser (a) and the QW DFB laser (b) as a function of the normalized bias current and measured at 283K, 293K and 303K. The black dashed lines indicate the minimum linewidth level at 283K and 303K.

However, experimental results also unveil that any further increase of the bias current leads to a linewidth rebroadening both for QD and QW lasers. The rebroadening refers to an increase of the linewidth with increasing bias current at high output power levels. In fact, the linewidth rebroadening occurs in any semiconductor lasers due to thermal effects, mode instability,[11] spatial hole burning,[12] and gain compression.[13,14] The first three of these effects are related to the device structure and can be minimized or eliminated by optimizing the laser design. For instance, a low grating coupling coefficient can reduce the effects of the spatial nonlinearities and so the spectral linewidth. Controlling the optical field distribution along the cavity through the facet coatings is also a way of eliminating the linewidth rebroadening. As for the gain compression, it is fundamentally related to the timescales for the carrier equilibrium dynamics in the semiconductor gain media and is usually enhanced in QD gain media. Therefore, as compared to QW lasers, the rebroadening can be actually more pronounced in QD lasers because of the increased scattering rates with the injected current and larger gain compression.[15,16] Indeed, experimental results show that the spectral linewidth of the QD DFB laser is raised by a factor of 1.8 at $2.8\times I_{th}$ (293 K) against 1.5 times at $5.4\times I_{th}$ for the QW DFB laser (293 K).

4. NUMERICAL SIMULATIONS

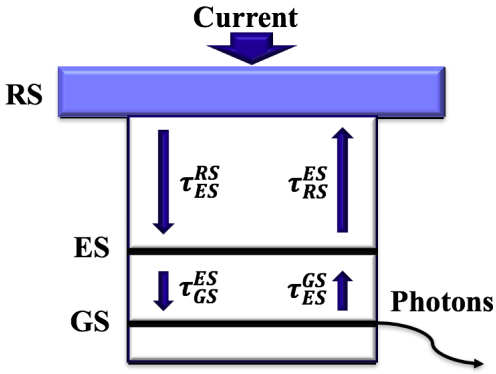

Figure 3. Schematic of the electronic structure and carrier dynamic in the InAs/InP QD structure.

The spectral linewidth of QD lasers is theoretically investigated through a differential rate equation model taking into account the spontaneous emission noise and the carrier noise. Figure 3 illustrates the electronic structure of the QD laser, where electrons and holes are treated as neutral excitons.[17] The QD ensemble includes two energy levels: a two-fold degenerate ground state (GS) and a four-fold degenerate excited state (ES). Carriers are supposed to be directly injected from contacts into the reservoir state (RS) so the carrier dynamics in the 3D barrier is not taken into account in the model. Stimulated emission occurs from the GS when the threshold is reached, and that from the ES is not considered in the model. Following Figure 3, the differential rate equation system describing carrier and photon dynamics is written such as:

$$\frac{dN_{RS}}{dt} = \frac{I}{q} + \frac{N_{ES}}{\tau_{RS}^{ES}} - \frac{N_{RS}}{\tau_{ES}^{RS}}(1-\rho_{ES}) - \frac{N_{RS}}{\tau_{RS}^{spon}} + F_{RS} \tag{7}$$

$$\frac{dN_{ES}}{dt} = (\frac{N_{RS}}{\tau_{ES}^{RS}} + \frac{N_{GS}}{\tau_{ES}^{GS}})(1-\rho_{ES}) - \frac{N_{ES}}{\tau_{GS}^{ES}}(1-\rho_{GS}) - \frac{N_{ES}}{\tau_{RS}^{ES}} - \frac{N_{ES}}{\tau_{ES}^{spon}} + F_{ES} \tag{8}$$

$$\frac{dN_{GS}}{dt} = \frac{N_{ES}}{\tau_{GS}^{ES}}(1-\rho_{GS}) - \frac{N_{GS}}{\tau_{ES}^{GS}}(1-\rho_{ES}) - \Gamma_p v_g g_{GS} S_{GS} - \frac{N_{GS}}{\tau_{GS}^{spon}} + F_{GS} \tag{9}$$

$$\frac{dS_{GS}}{dt} = (\Gamma_p v_g g_{GS} - \frac{1}{\tau_p}) S_{GS} + \beta_{sp}\frac{N_{GS}}{\tau_{GS}^{spon}} + F_S \tag{10}$$

$$\frac{d\phi}{dt} = \frac{1}{2}\Gamma_p v_g (g_{GS}\alpha_H^{GS} + g_{ES}\kappa_{ES} + g_{RS}\kappa_{RS}) + F_\phi \tag{11}$$

where N_{RS}, N_{ES} and N_{GS} are the carrier populations in the GS, ES, and RS respectively, while S_{GS} accounts for the photon population in the GS level. In order to retrieve the spectral linewidth, the phase of the electric field (ϕ) is also included. In Eqs. (7) - (11), τ_{ES}^{RS} is the carrier capture time from RS into ES. The carriers then relax from the ES to the GS with a relaxation time τ_{GS}^{ES}. Conversely, some carriers will escape from the GS to the ES with an escape time τ_{ES}^{GS}, and from the ES to the RS with an escape time τ_{RS}^{ES} through thermal excitations. $\tau_{RS,ES,GS}^{spon}$ are the spontaneous emission times, τ_p is the photon lifetime, v_g is the group velocity of light. The gain of each state is expressed as $g_{RS,ES,GS}$ while $\rho_{RS,ES,GS}$ represent the carrier occupation probabilities in the RS, ES, and GS. α_H^{GS} is the contribution of the GS carriers to the phase-amplitude coupling factor (α_H - factor), and the coefficients $\kappa_{ES,RS}$ are defined in.[18] The frequency noise (FN) in semiconductor lasers is contributed from the spontaneous emission noise, the carrier generation and recombination noises, as well as the low-frequency flicker noise. In the model, carrier recombination noises are considered through the Langevin noise sources $F_{RS,ES,GS}$ to the carrier numbers in Eqs. (7) - (9). Additionally, the spontaneous emission noise of the laser light is expressed as F_S to the photon number in Eq. (10) and F_ϕ to the phase in Eq. (11). In this paper, the contribution of the flicker noise, such as the electrical noise from the pump current source, temperature variations, and mechanical vibrations, is not considered in this model. Derivations of auto- and cross-correlations

terms will be reported elsewhere. Using a small-signal analysis of Eqs. (7) - (11), the FN of the laser is calculated by $\mathrm{FN}(\omega) = |j\omega\delta\phi(\omega)/2\pi|^2$ with $\delta\phi(\omega)$ being the phase fluctuation due to the noise perturbation. All material and optical parameters used in the simulations are listed in Table 1.[17] The laser threshold current is calculated to be 48 mA at 293K. The spectral linewidth of the QD laser is then extracted from the FN spectrum at low frequencies as $\Delta\upsilon = 2\pi FN(\omega \to 0)$.

Table 1. Material and laser parameters used in the simulations.

Symbol	Description	Value
E_{RS}	RS transition energy	0.97 eV
E_{ES}	ES transition energy	0.87 eV
E_{GS}	GS transition energy	0.82 eV
τ_{ES}^{RS}	RS to ES capture time	6.3 ps
τ_{GS}^{ES}	ES to GS relaxation time	2.9 ps
τ_{RS}^{ES}	ES to RS escape time	10 ns
τ_{ES}^{GS}	GS to ES escape time	10 ps
τ_{RS}^{spon}	RS spontaneous emission time	0.5 ns
τ_{ES}^{spon}	ES spontaneous emission time	0.5 ns
τ_{GS}^{spon}	GS spontaneous emission time	2.8 ns
τ_p	Photon lifetime	6.3 ps
T_2	Polarization dephasing time	0.1 ps
β_{sp}	Spontaneous emission factor	0.8×10^{-4}
a_{GS}	GS Differential gain	5.0×10^{-15} cm^2
a_{ES}	ES Differential gain	10×10^{-15} cm^2
a_{RS}	RS Differential gain	2.5×10^{-15} cm^2
ξ	Gain compression factor	2.0×10^{-16} cm^3
Γ_p	Optical confinement factor	0.06
α_H^{GS}	GS contribution to α_H-factor	0.5
N_B	Total dot number	6.0×10^7
D_{RS}	Total RS state number	7.2×10^6
V_B	Active region volume	7.5×10^{-11} cm^3
V_{RS}	RS region volume	1.5×10^{-11} cm^3

Figure 4 presents the evolution of the spectral linewidth as a function of the normalized bias current between 283 K and 303 K. Overall, the simulation well reproduces the experimental results except the linewidth rebroadening. The latter can not be predicted because of the various assumptions made in the model. Indeed, flicker noise, gain compression and spatial hole burning are not taken into account at this stage.[16] Nevertheless, for a bias current of 155 mA, the calculated spectral linewidth increases from 170.5 kHz ($I/I_{th} = 3.4$) at 283K to 175.1 kHz ($I/I_{th} = 3.2$) at 293K, and 179.8 kHz ($I/I_{th} = 3.1$) at 303 K which is in agreement with the measured values. The simulation also confirms that the spectral linewidth of QD lasers is rather insensitive to the temperature range.

5. CONCLUSIONS

In summary, we have investigated both experimentally and theoretically the temperature dependence of the spectral linewidth of InAs/InP QD DFB lasers. By comparison with QW lasers, we show that the spectral

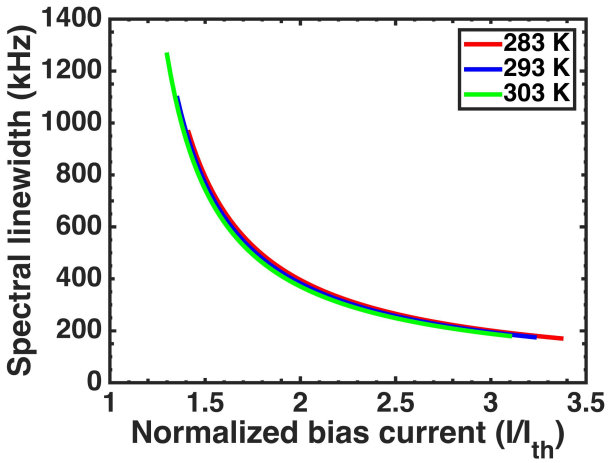

Figure 4. Spectral linewidth of the QD DFB laser as a function of the normalized bias current and calculated at 283K, 293K and 303K.

linewidth of QD lasers is rather insensitive to the temperature with minimum values below 200 kHz between 283 K and 303 K. In addition, the numerical simulations based on differential rate equations nicely reproduces the temperature behavior. Such results indicate that QD lasers are excellent candidates for narrow linewidth operation, which is of first importance not only for coherent communication systems but also for high-resolution spectroscopy, high purity photonic microwave generation and on-chip atomic clocks.

ACKNOWLEDGMENTS

This work is supported by the European Office of Aerospace Research and Development (EOARD) under grant FA9550-15-1-0104. J. Duan's work is supported by China Scholarship Council.

REFERENCES

[1] Kikuchi, K., "Fundamentals of coherent optical fiber communications," *Journal of Lightwave Technology* **34**(1), 157–179 (2016).

[2] Seimetz, M., "Laser linewidth limitations for optical systems with high-order modulation employing feed forward digital carrier phase estimation," in [*Optical Fiber communication/National Fiber Optic Engineers Conference, 2008. OFC/NFOEC 2008. Conference on*], 1–3, IEEE (2008).

[3] Kapon, E., [*Semiconductor lasers I: fundamentals*], Academic Press (1999).

[4] Crowley, M. T., Naderi, N. A., Su, H., Grillot, F., Lester, L. F., and Bryce, A., "GaAs-based quantum dot lasers," *Advances in Semiconductor Lasers* **86**(371), 42 (2012).

[5] Lu, Z., Poole, P., Liu, J., Barrios, P., Jiao, Z., Pakulski, G., Poitras, D., Goodchild, D., Rioux, B., and SpringThorpe, A., "High-performance 1.52 μm InAs/InP quantum dot distributed feedback laser," *Electronics letters* **47**(14), 818–819 (2011).

[6] Becker, A., Sichkovskyi, V., Bjelica, M., Rippien, A., Schnabel, F., Kaiser, M., Eyal, O., Witzigmann, B., Eisenstein, G., and Reithmaier, J., "Widely tunable narrow-linewidth 1.5 μm light source based on a monolithically integrated quantum dot laser array," *Applied Physics Letters* **110**(18), 181103 (2017).

[7] Duan, J., Huang, H., Schires, K., Lu, Z., Poole, P. J., and Grillot, F., "Narrow linewidth quantum dot distributed feedback lasers," in [*Compound Semiconductor Week (CSW/IPRM), 2017 and 29rd International Conference on Indium Phosphide and Related Materials*], C7.4 (2017).

[8] Bimberg, D., Kirstaedter, N., Ledentsov, N., Alferov, Z. I., Kop'Ev, P., and Ustinov, V., "InGaAs-GaAs quantum-dot lasers," *IEEE Journal of selected topics in quantum electronics* **3**(2), 196–205 (1997).

[9] Okoshi, T., Kikuchi, K., and Nakayama, A., "Novel method for high resolution measurement of laser output spectrum," *Electronics letters* **16**(16), 630–631 (1980).

[10] Thompson, P., Cox, D., and Hastings, J., "Rietveld refinement of Debye-Scherrer synchrotron X-ray data from Al_2O_3," *Journal of Applied Crystallography* **20**(2), 79–83 (1987).

[11] Olesen, H., Tromborg, B., Lassen, H., and Pan, X., "Mode instability and linewidth rebroadening in DFB lasers," *Electronics Letters* **28**(5), 444–446 (1992).

[12] Takaki, K., Kise, T., Maruyama, K., Yamanaka, N., Funabashi, M., and Kasukawa, A., "Reduced linewidth re-broadening by suppressing longitudinal spatial hole burning in high-power 1.55 μm continuous-wave distributed-feedback (CW-DFB) laser diodes," *IEEE journal of quantum electronics* **39**(9), 1060–1065 (2003).

[13] Agrawal, G., Duan, G.-H., and Gallion, P., "Influence of refractive index nonlinearities on modulation and noise properties of semiconductor lasers," *Electronics Letters* **28**(19), 1773–1774 (1992).

[14] Girardin, F., Duan, G.-H., and Gallion, P., "Linewidth rebroadening due to nonlinear gain and index induced by carrier heating in strained quantum-well lasers," *IEEE Photonics Technology Letters* **8**(3), 334–336 (1996).

[15] Melnik, S., Huyet, G., and Uskov, A. V., "The linewidth enhancement factor α of quantum dot semiconductor lasers," *Optics Express* **14**(7), 2950–2955 (2006).

[16] Redlich, C., Lingnau, B., Huang, H., Raghunathan, R., Schires, K., Poole, P., Grillot, F., and Lüdge, K., "Linewidth rebroadening in quantum dot semiconductor lasers," *IEEE Journal of Selected Topics in Quantum Electronics* **23**(6), 1–10 (2017).

[17] Wang, C., Zhuang, J.-P., Grillot, F., and Chan, S.-C., "Contribution of off-resonant states to the phase noise of quantum dot lasers," *Optics express* **24**(26), 29872–29881 (2016).

[18] Wang, C., Osiński, M., Even, J., and Grillot, F., "Phase-amplitude coupling characteristics in directly modulated quantum dot lasers," *Applied Physics Letters* **105**(22), 221114 (2014).